Composites Part B 128 (2017) 146–154

Contents lists available at ScienceDirect

Composites Part B

journal homepage: www.elsevier.com/locate/compositesb

Enhancing mechanical properties of bolted carbon/epoxy nanocomposites with carbon nanotube, nanoclay, and hybrid loading

Mehmet Çağrı Tüzemen [a, *], Elmas Salamcı [a], Ahmet Avcı [b]

[a] Department of Mechanical Engineering, Faculty of Engineering, University of Gazi, Ankara, Turkey
[b] Department of Mechanical Engineering, Faculty of Engineering, University of Selçuk, Konya, Turkey

ARTICLE INFO

Article history:
Received 13 March 2017
Received in revised form
21 June 2017
Accepted 1 July 2017
Available online 1 July 2017

Keywords:
Carbon fiber
Nanostructures
Mechanical properties
Joints

ABSTRACT

The effects of adding nanoclay (NC), carbon nanotube (CNT), and a hybrid of both on bending, tensile and bearing strengths of nanocomposite plates were investigated in this study. Sonication method was used to ensure dispersion of the nanoparticles in epoxy homogeneously. The nanocomposite plates were produced by a vacuum assisted resin transfer molding (VARTM) process. Mechanical properties were investigated by applying bending and tensile testing as well as tensile test with bolted joints on the nanocomposite plates. According to the bearing strength, 5.2%, 3.9%, and 0.8% improvements were obtained in NC, CNT and hybrid (NC + CNT) loaded specimens respectively while much more improvement range from 47.7% to 57.1% was obtained in tensile strength. In addition, the impact of nanoparticle loading on the porosity was determined by applying the burning test and its effect on the mechanical properties was discussed.

1. Introduction

The use of composite materials is becoming widespread increasingly and this has led to different applications of composite materials under various circumstances [1–7]. One of these different circumstances is mechanical connection of two composite materials with bolt. Moreover, nanotechnology has recently been utilized to develop mechanical and physical properties of composite materials. Loading of nanoparticles in the matrix material has become a commonly used method for this reason [8–11].

Over the past few years, remarkable research have been directed toward joints in composite materials. Mechanical joints and adhesively bonded joints are two main types of joints in composite materials. The latter is strongly affected by the environment like humidity or temperature [12]. Mechanical joints are detachable joints unlike adhesively bonded joints. Common bearing test failure modes of composite bolted joints are net-tension, shearout, bearing, tearout, cleavage, and fastener failure. These damage modes depends on joint geometry, fiber inclination angle, matrix and fiber type, and stacking sequence of the laminates [13–19]. Although there are a lot of literature on application of nanoparticles in composites but studies related to detachable connections in nanocomposites are still limited. Furthermore, there is only one study regarding the bolted joint with nanoparticle loading. In this study, carbon nanotubes (CNT) networks were used instead of nanoparticles [15]. No NC or hybrid loading was found to be used in previous studies related to bolted joint in composites [16–19]. In previous research regarding to adhesively bonded joints in nanocomposite structures, CNT were used instead of nanoparticles [20–23].

Friedrich et al. investigated the failure modes of the mechanically connected composites in their study [15]. Thostenson et al. investigated failure mode and electrical conductivity of mechanically connected composites with CNT loading [24]. However, in both studies, the CNT loading was used to change the conductivity of the material but its effects on mechanical properties were not investigated.

Commonly two types of nanoparticles are added in the matrix to enhance the mechanical properties of the composite material, CNT and NC. Although there have been numerous studies conducted on CNT, studies related to NC and a hybrid of both CNT and NC (the hybrid from this point on) have been limited. These limited numbers of studies have shown discrepancy regarding the optimal

* Corresponding author.
E-mail address: cagrituzemen@gazi.edu.tr (M.Ç. Tüzemen).

http://dx.doi.org/10.1016/j.compositesb.2017.07.001
1359-8368/

percentage of NC loading for the most effective way to improve mechanical properties. In several studies, the NC loading up to 5 wt % increased tensile strength, compressive strength and elastic modulus [25–28]. While some studies revealed that 3 wt% of NC loading was the optimum fraction to increase the mechanical properties [29,30], other studies showed that NC loading should be between 2 wt% and 5 wt% [31–36].

In this study, the mechanical properties of NC (4 wt%), CNT (0.3 wt%) and the hybrid (4 wt% NC and 0.3 wt% CNT) reinforced nanocomposite plates with bolted joint were investigated. The impact of different nanoparticles loading on the mechanical properties and particularly on the bearing strength were investigated and compared with the relevant studies in the literature. Loading of NC showed the highest bearing strength as well as toughness.

2. Experimental

2.1. Materials

Carbon was used as fiber, epoxy was used as matrix material, NC and CNT was used as nanoparticles. Four different specimens were prepared, neat, 4 wt% NC (NC4), 0.3 wt% CNT (CNT3) and the hybrid (4 wt% NC and 0.3 wt% CNT). (see Table 1, Fig. 1)

2.2. Nanocomposite plate production by using VARTM

Vacuum infusion process was used in the nanocomposite plate production in our study according to the reported studies [15,37,38]. All the composite plates were fabricated with seventeen equally oriented wowen fabric layers which has same mechanical properties both 0° and 90° directions.

Uniform dispersion of NC and CNT in the epoxy to avoiding the agglomeration of the particles is a case to be handled. For this reason, the probe sonication method, commonly used in the literature, was used [27,28]. It enables dispersion of NC and CNT in the epoxy by means of creating high and low pressure areas within the epoxy itself. The increase in the duration of sonication results in an increase in the temperature of the epoxy. Overheating may damage the epoxy. Therefore, the epoxies should be cooled during sonication [39]. In this study, the sonication periods were divided into parts (4 × 10 min out of 40 min) and thus shortened to avoid overheating. Overheating has two advantages: a decrease in the viscosity and a reduction in the quantity of the air bubbles in the epoxy.

Hardeners were added in the prepared resins at a ratio of 4:1. After the hardener was mixed well inside the epoxy, the epoxy should be absorbed by the fibers before curing starts. The absorption of the nanoclays by the fibers is as important as their dispersion in the epoxy. In this method, a non-wetting phenomenon is a frequently faced problem [40].

Table 1
Mechanical properties of the materials used.

	Tensile Strength [MPa]	Elongation [%]	Elastic Modulus [GPa]
Carbon Fiber	3950	1.7	238
Epoxy	70–80	5–6.5	3–3.3

2.3. Burning test

The burning test was performed in accordance with American Society for Testing and Materials (ASTM) D 2734 and D 2584 standards. The test was done to determine the fiber and matrix volume fractions and porosity in the produced nanocomposite specimens. Porosity is especially a determining factor to ensure a reliable production. Therefore, this fraction has an important role in terms of understanding tensile and bending test results. In addition, the burning test was done to determine whether the nanoparticles loading had an effect on the volume fractions or not. First of all, the specimens were cut in accordance with the standard measurements and their volumes were calculated for each test. Before proceeding with the burning test, the specimens were weighed and total mass was determined. Following this process, the specimens were burned at approximately 565 °C in the furnace to remove epoxy from the composite and remaining fibers thereof were reweighted and noted down. By considering the densities, the volumes of used fiber and epoxy materials were calculated and finally the void volume fraction was determined by subtracting the calculated volumes from the total volume.

2.4. Three point bending test

The three point bending test was carried out in accordance with the standards of ASTM D7264/D7264 M. This test was performed to determine the flexural strength properties of the polymer matrix composites. All the specimens were tested at 1 mm/min in accordance with the standards.

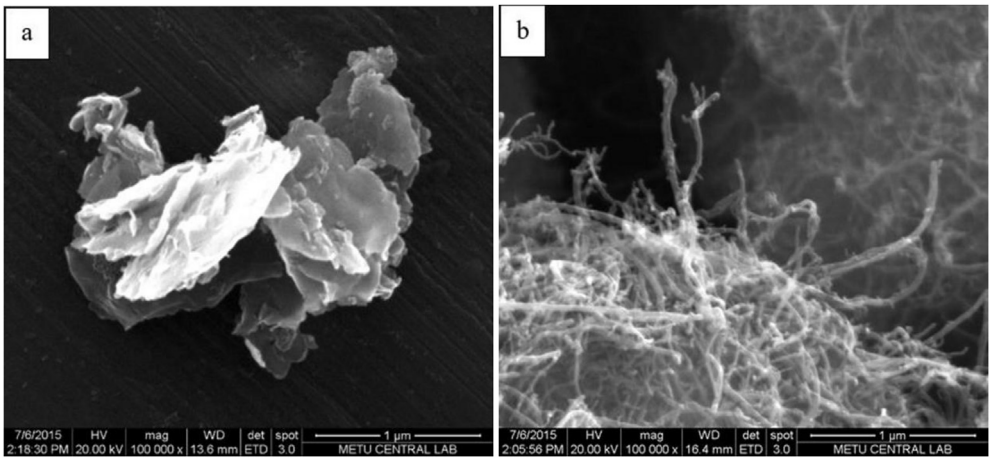

Fig. 1. SEM images of the nanoparticles used in this study (a) NC (b) CNT.

2.5. Tensile test

Tensile test was performed in accordance with the standards of ASTM D3039/D3039 M. This test method was carried out to determine the tensile strength of the polymer matrix composite materials reinforced with fibers of high elastic modulus such as carbon. The length and width of the specimens were 250 mm and 25 mm, respectively, as specified in the standards. The test was performed at 2 mm/min.

2.6. Tensile test of bolted joints

Tensile testing of bolted joints was performed in accordance with the standards of ASTM D5961/5961 M. The tests were carried out in the Instron testing machine. This test was performed to define the bearing strength results of the polymer matrix composites with bolted joints reinforced with fibers of high elastic modulus. The method used in the present study is two unsupported specimens with single lap bolted joint are exposed to tensile strength. The test speed was set as 2 mm/min.

The doublers having the same thickness as the specimens were placed between the specimen and grip for the force to pass exactly through the attachment point of the specimens so as to avoid bending and thus forming different forces. The bolts specified in the standards were used as connector. Half thread bolts were used to prevent a possible damage arising from the bolt threads in the connection point to the composite material. Lock nut was used to avoid loosening of the bolt connection. Furthermore, unwanted damages to the material due to bolt head or bolt or even the washers themselves were avoided by means of placing washer of adequate sizes between bolt head-specimen and between locknut-specimen. The bolts, lock nuts, and washers were not reused. (see Fig. 2, Table 2)

Table 2
Dimensions of the specimens.

Parameters	Dimensions (mm)
Hole diameter, D	6 + 0.03/-0.00
Thickness, h	3.63
Length, L	135
Width, w	36 ± 1
Edge distance, e	18 ± 1
Doubler length, s	75

3. Results and discussion

3.1. Volume fractions

Fiber, matrix and void volume fractions of the produced nanocomposite plates were determined with the burning test. The effect of nanoparticles loading on the epoxy density enabled a more reliable determination of the volume fractions, for a loading of 10% NC by weight (10 wt%) increased the density of epoxy by 3% [30]. The epoxy density for each specimen was calculated separately in the light of this information. Fiber volume fraction (FVF) of neat composite plates produced by VARTM is higher than that of a hand lay-up and hot isostatic pressing (HIP) techniques [42,43]. The volume fractions of the produced specimens were shown in Table 3. V_f indicates FVF, V_m indicates matrix volume fraction (MVF) and V_v indicates void volume fraction (VVF).

There are two important points to be brought into attention: the decrease in the FVF and increase in the VVF with the increasing quantity of nanoparticles. It could be attributed to increasing the viscosity of the matrix [39]. This increase in the viscosity may lead to less suction of extra epoxy under the vacuum during the production compared to the neat. Thus, the MVF within the composite structure was increased.

Uniform dispersion of nanoparticles in the matrix is an important issue. The increase in the VVF in proportion to the nanoparticles loading can be explained by agglomeration of nanoparticles. As a conclusion, the nanoparticles behave as a barrier by forming agglomeration in the matrix while epoxy wets the fibers during the production and thus leading to small air gaps in the composite structures.

3.2. Flexural properties

The behaviors of the nanocomposite specimens reinforced with nanoparticles under the flexural load were examined by doing the three point bending test (Table 4).

Both NC and CNT loading increased the flexural strength of

Table 3
Volume fraction of nanocomposite plates.

	V_f	V_m	V_v
Neat	70.72	28.24	1.04
NC4	67.24	30.74	2.02
CNT3	69.90	28.91	1.20
Hybrid	66.98	31.03	1.99

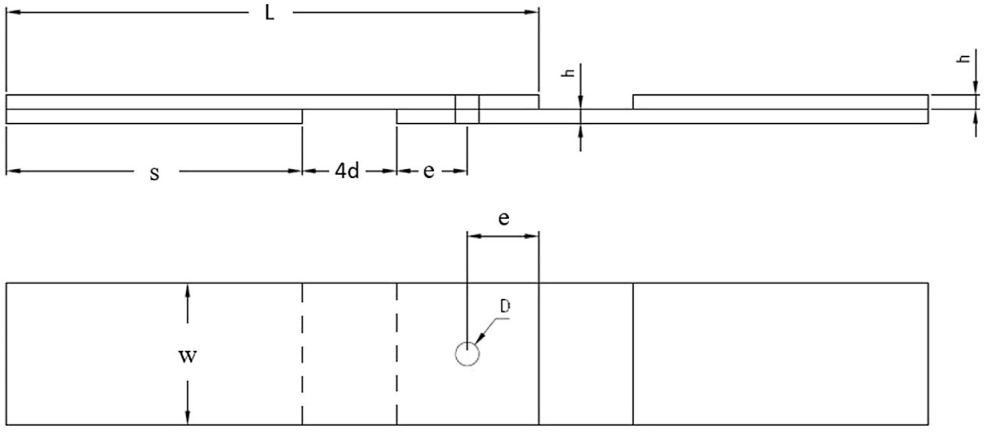

Fig. 2. Single shear, two-piece single-fastener test specimen drawing [41].

Table 4
Flexural properties of nanocomposite plates.

	Flexural Strength (MPa)	Strain (mm/mm)	Flexural Elastic Modulus (GPa)	Toughness (MJ/m^3)
Neat	277	0.055	5.09	7.92
NC4	334	0.056	7.82	9.68
CNT3	353	0.053	6.91	9.76
Hybrid	278	0.051	8.22	8.93

nanocomposite plates compare to the neat one. Contrary to this, it was reported that flexural strength decreases with NC loading [44]. Flexural strength decreases and flexural elastic modulus increases with the hybrid loading compared to CNT and NC loading. Contradictory results were found in the literature [45,46]. Flexural elastic modulus and toughness increases with NC and CNT loading in line as reported in previous study [44–46]. The hybrid plates may have reached lower mechanical properties than those NC or CNT plates due to agglomeration, excessive amount of nanoparticles loading or interfere with each other's properties.

The strain values are lower than that of neat specimen in CNT3 and the hybrid specimens. This could have arisen from that NC behave as a barrier against the crack propagation by means of increasing the crack length. This case may also be a significant mechanism for increasing the toughness. In addition, the bridging effect formed in the cracked areas of the nanoclays may be regarded as another mechanism to increase the toughness. In the literature, similar results have been observed [47,48].

Consequently, the nanoparticles loading increases the flexural strength of the nanocomposites (Fig. 3). The highest increase is in the CNT3 specimen and almost no increase in the hybrid one. Fluctuations was observed close to the fracture point (Fig. 3) due to the breaking fibers on the surface exposed to tension stresses (Fig. 4b).

Fig. 4 illustrates the macro and micro views of failure surfaces of the NC loaded specimen exposed to the three point bending test. The arrows in Fig. 4(b) shows the direction of the applied force, the compression and tension forces which occur as a result of the applied force. Fig. 4(c) demonstrates the delamination of the layers as a consequence of compression force. The epoxy tries to form bridge between the layers to prevent delamination. This may be interpreted as there is an agreeable adhesion between the epoxy and carbon fiber.

In Fig. 5, the cross section of the NC loaded specimen's failure area following the three point bending test has been shown. The arrows in Fig. 5(a) shows the same forces as in Fig. 4(b). In Fig. 5(b), three different types of failure can be seen: delamination, fiber rupture, and fiber fragmentation.

3.3. Tensile properties

The behavior of the nanocomposites reinforced with nanoparticles under axial tension were examined with the tensile test. Table 5 shows the results of the tensile test. Toughness could be explained as an ability of a material to absorb energy before it is fractured. The highest increase in the toughness was obtained in the NC4 specimen with an increase of over 107%. In other words, the absorbed energy in the specimen with NC loading of 4% by weight increased more than twice as that of the neat specimen. Although the hybrid has 4 wt% NC, the toughness is lower than NC4 and CNT3. Tensile strength and elastic modulus increases with nanoparticle loading in line with the previous studies [25,26,28,29]. Contrary to this, it was reported in some previous studies that ultimate strength decreases with CNT or the hybrid loading [46,49].

Fracture behavior of the fiber-reinforced composite materials consists of two stages (Fig. 6). In the initial Stage I region, both

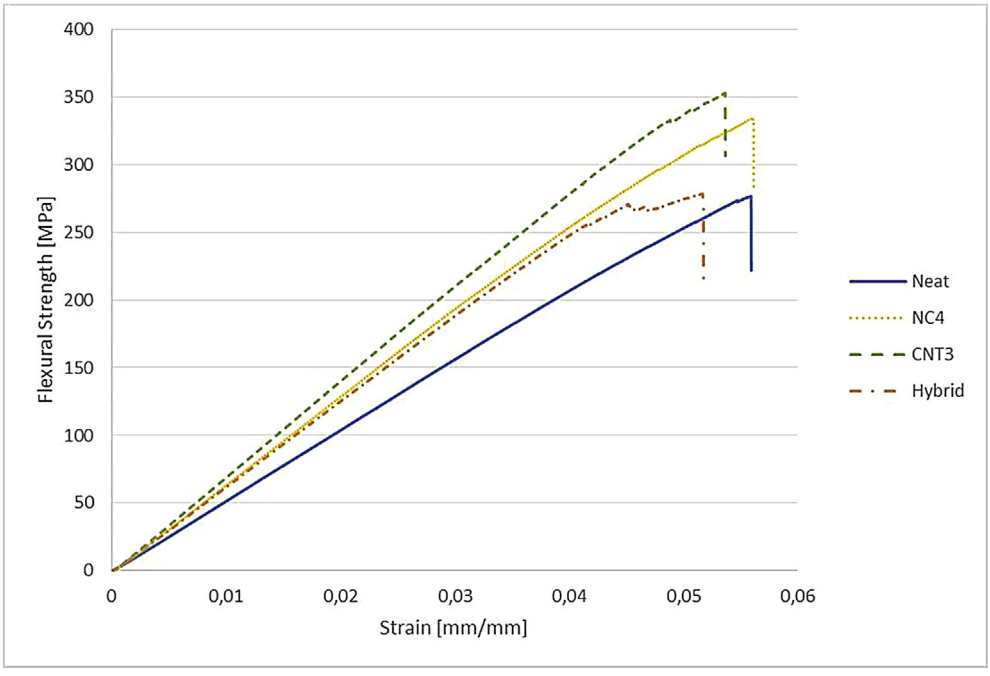

Fig. 3. Flexural strength/strain curve of nanocomposites.

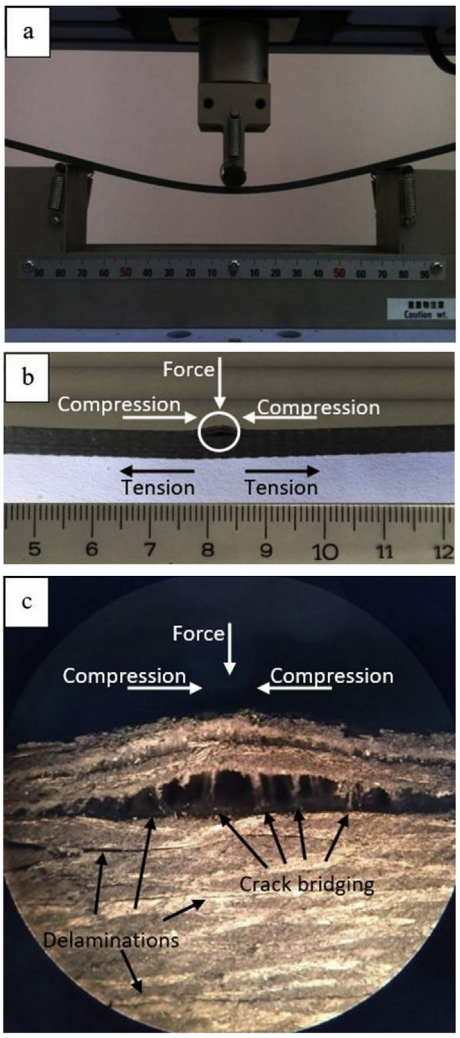

Fig. 4. (a) Three-point bending setup (b) macro (b) micro (30x) view of the delaminated area of the NC loaded specimen after test.

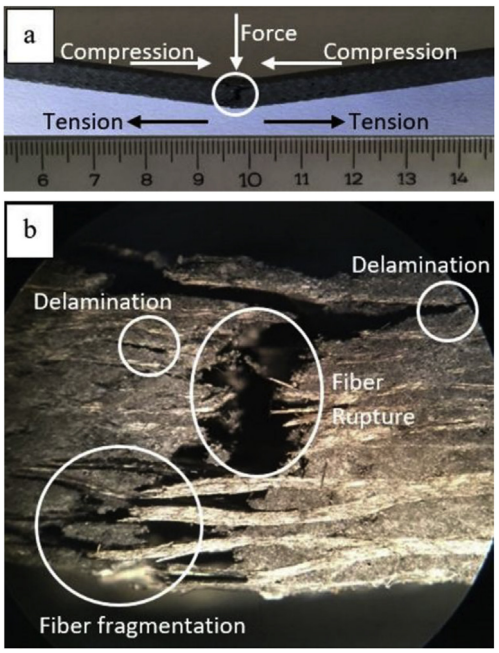

Fig. 5. (a) Macro (b) micro (30x) view of multiple failure modes area of the NC loaded specimen after three-point bending test.

fibers and matrix deform elastically. In Stage II region, as the tensile strength of fiber significantly higher than the yield strength of the matrix, the matrix yields and deforms plastically while the fibers continue to stretch elastically. Normally, the curves in the Stage I region are linear and the curves in the Stage II region are very nearly linear but of diminished slope relative to Stage I [50].

3.4. Bearing properties

Bearing strength of the nanoparticle reinforced nanocomposite plates under the axial load was examined with tensile testing of bolted joints. Common bearing test failure modes and test specimen before and after the bearing test has been shown in Fig. 7 and Fig. 8, respectively. All the specimens of the bearing test showed the shearout failure mode (Fig. 8).

The bearing strength, elastic modulus and toughness increases by nanoparticle loading (Fig. 9). Bearing strain increases by NC loading but decreases by CNT loading (Table 6).

Test results in Fig. 10 indicated bearing strength-bearing strain curves. In this figure, there are two attention-grabbing matters. One is that upon the application of the load, there is an instantaneous horizontal movement of the curves at the very beginning of the graphic. This movement is associated with the elimination of the frictions formed in the joint areas and the voids occurred due to the hole tolerance. The second matter is the fluctuations on the graphics. This may be caused by local layer delamination which results in crack formation in the matrix after the bearing failure starts. Similar results were also obtained in the literature [52].

Just as in the bending tests, herein as well, the least increase in bearing strength was observed in the hybrid loading. In this regards, there are three reasons for this behavior. The first one is decreasing in the FVF and increasing in the VVF in the matrix during the production. As a result, these voids raises the stress in the composite structure and behave like a crack. Hence, the voids decrease the strength under the load conditions. The second one is that the increasing nanoparticle loading which causes agglomeration even after the sonication. The third one is the filtration effect on the fiber cloth during the epoxy absorption by the fibers. The agglomeration behaves as stress raiser like air gaps.

While nanoparticles loading increased the bearing strength, it was not as influential as the tensile or bending tests. Bearing strength was also affected by the drilled holes for the bolt joints in the specimens. Drilled holes also lead to stress concentrations as air gaps and nanoparticle agglomeration. Because the hole has the smallest cross section in the specimen, the damage occurs in these most vulnerable areas. These mentioned air gaps and nanoparticle agglomeration may occur near the hole, even on the hole surface. Therefore, the area around the hole of the specimen would be weakened and more susceptible to damage under loading. As a result, the nanoparticles loading in the bearing test less increases the strength comparing the bending and tensile tests.

SEM images of the failure areas of the NC reinforced and neat specimens are illustrated in Fig. 11. In the NC reinforced specimens, NC4 (Fig. 11b), the matrix much better adheres to the fiber; thus, there is a good bonding force compared to the neat specimens (Fig. 11a). Furthermore, since the epoxy residues on the fiber are less in the neat specimen, the fibers could be separated from the matrix easily. The addition of NC to the specimens creates a strong bonding force between the fiber and epoxy. The residue epoxies on the fibers which are pulled out from the matrix in the NC4

Table 5
Tensile properties of nanocomposite plates.

	Tensile Strength (MPa)	Ductility, %EL	Elastic Modulus (GPa)	Toughness (MJ/m^3)
Neat	396	2,3	33,093	5,91
NC4	585	3,2	36,784	12,27
CNT3	610	3,1	38,091	11,50
Hybrid	622	2,9	37,794	10,42

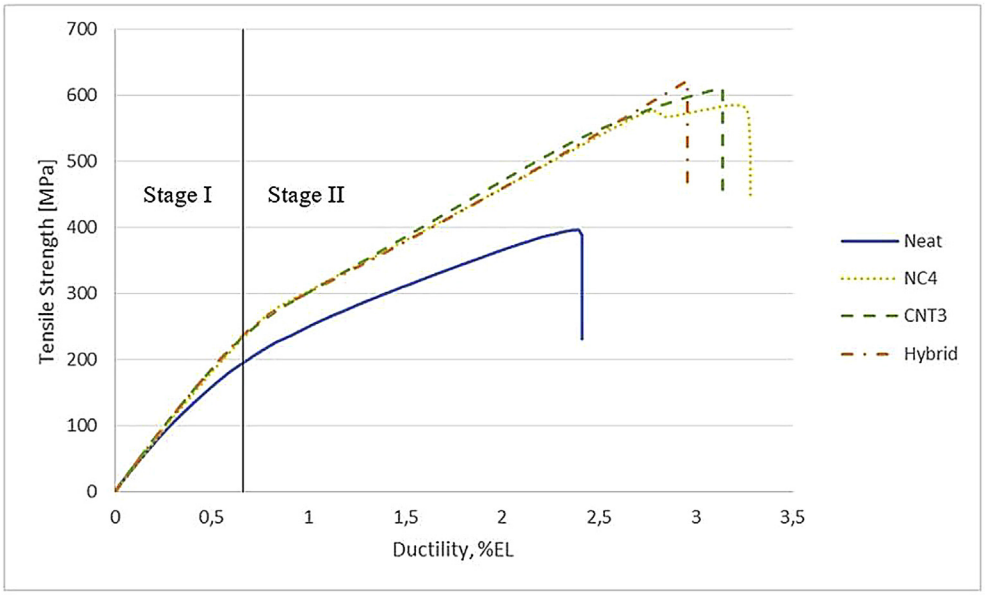

Fig. 6. Tensile strength/ductility curve of nanocomposites.

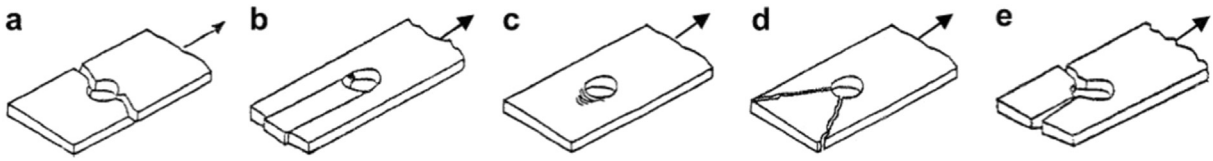

Fig. 7. Common bearing test failure modes (a) lateral (net-tension), (b) shearout, (c) bearing, (d) tearout and (e) cleavage [51].

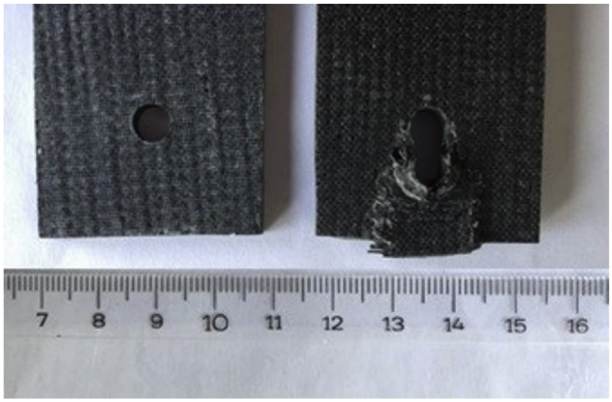

Fig. 8. The specimen before and after the bearing test and shearout failure mode occurred in the entire specimens.

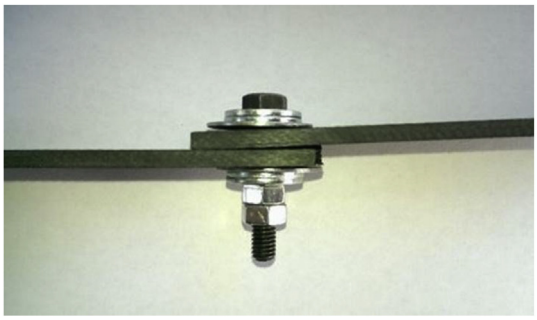

Fig. 9. Side view of the specimen after bearing test. Lock nut was used to avoid loosening of the bolt connection.

specimen can be seen in Fig. 11(b) are the evidence of strong bonding force. Smooth fracture surfaces in Fig. 11(a) shows the brittle fracture mode of neat specimen and rough fracture surfaces of NC loaded specimen in Fig. 11(b) indicates that fracture mode changes from brittle to ductile.

In Fig. 12(a) SEM images of the agglomerated NC used in this study and NC loaded specimen (Fig. 12b) are illustrated. Encircled area indicate possible NC standing on the matrix crack way and crack bridging. Spaces can be observed in the pullout area (Fig. 12b)

Table 6
Bearing properties of nanocomposite plates.

	Bearing strength (MPa)	Bearing Strain, %	Bearing Elastic Modulus (GPa)	Toughness (MJ/m^3)
Neat	510	44,9	3871	236,50
NC4	537	47,9	4378	275,66
CNT3	530	44,7	3941	272,33
Hybrid	514	49,1	4575	237,20

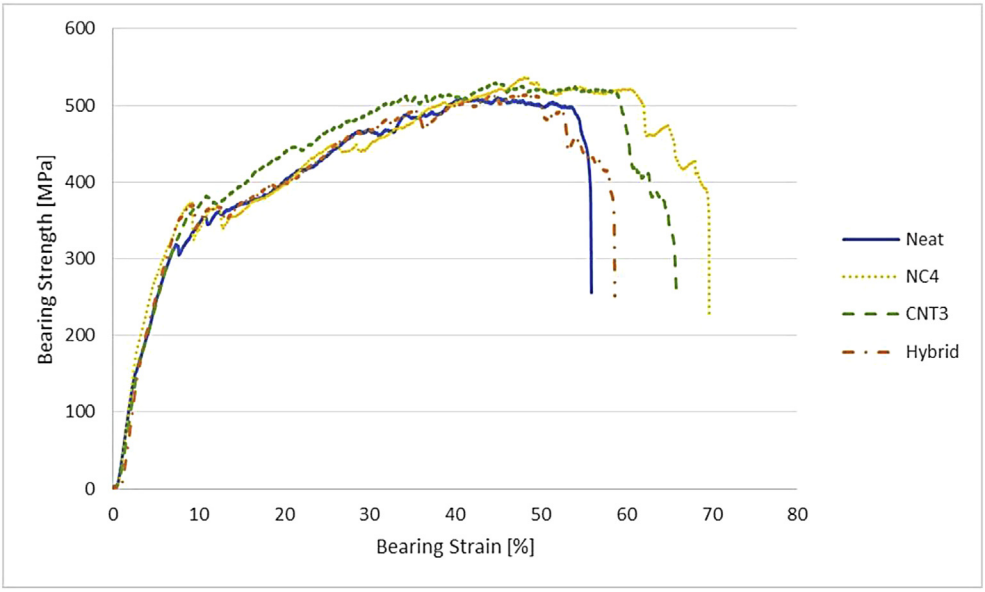

Fig. 10. Bearing strength/bearing strain curves of nanocomposites.

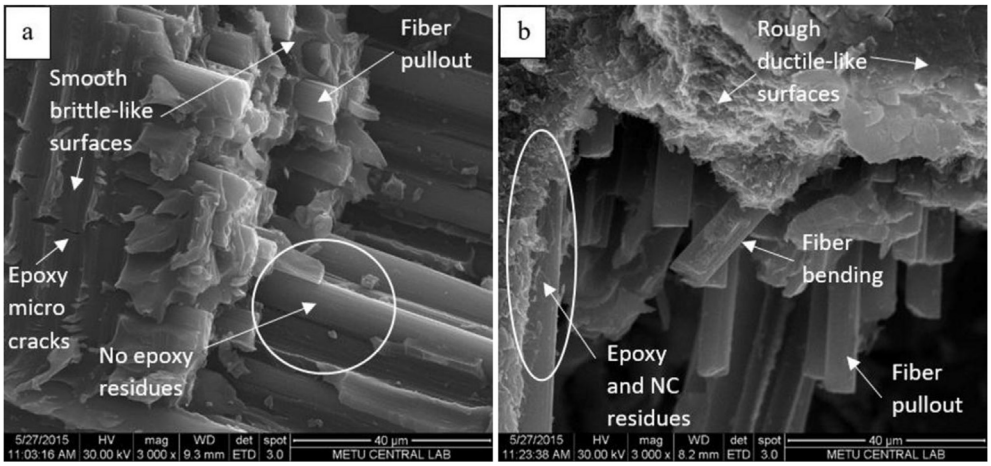

Fig. 11. SEM images of (a) neat specimen shows brittle-like epoxy surface and weak fiber-matrix interfacial strength (b) NC4 specimen shows ductile-like epoxy surface and strong fiber-matrix interfacial strength.

and these spaces decrease the bonding force. Fig. 13 illustrated the single CNT bridging the matrix cracks which shows how the CNT enhancing the strength of nanocomposite plates.

4. Conclusions

The FVF decreases and the VVF increases with an increase in the wt.% of nanoparticles. The increase in the viscosity of the matrix led to less suction of epoxy residues under the vacuum during the production compared to the neat specimens. Therefore, it was concluded that the MVF increased while the FVF decreased in the composite structure.

The hybrid specimens showed lower flexural and bearing strength compare to NC4 and CNT3 specimens. This might be due to excessive amount of nanoparticles loading, agglomeration or interfere with each other's properties. For further development of this study NC and CNT can be mixed at different ratios to obtain hybrid samples with higher strength. The flexural strength increased with the addition of nanoparticle. The increase was high for NC and CNT addition while it was low for the hybrid.

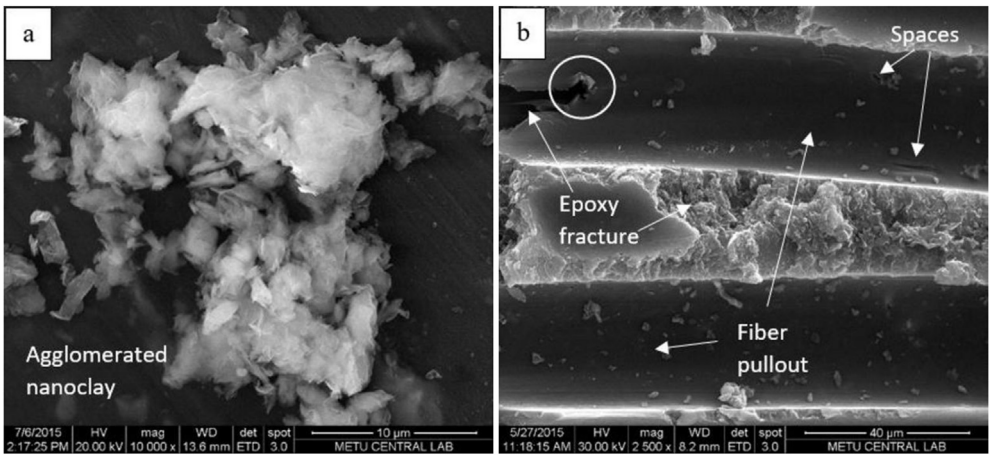

Fig. 12. SEM images of (a) agglomerated nanoclay (b) epoxy matrix of the nanoclay loaded composite. Encircled area indicate possible nanoclay standing on the matrix crack way and crack bridging.

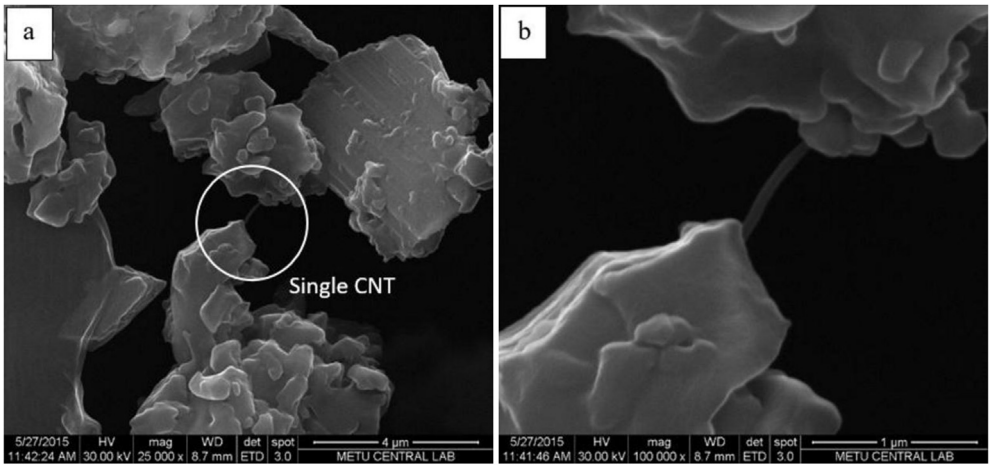

Fig. 13. CNT bridging matrix cracks of CNT3 specimen (a) 25000 x (b) 100000× magnification.

The behaviors of the nanocomposite specimens with bolted single lap joint under the axial tensile load were examined with the tensile testing of bolted joints. The maximum increase in the bearing strength was obtained from the NC loaded and the least increase is obtained from the hybrid loaded specimens. Bearing strain increases with NC and the hybrid loading but decreases with CNT loading. Both bearing elastic modulus and toughness increases with nanoparticle loading.

References

[1] Berardi VP, Perrella M, Feo L, Cricrì G. Creep behavior of GFRP laminates and their phases: experimental investigation and analytical modeling. Compos Part B 2017;122:136–44.
[2] Colangelo F, Russo P, Cimino F, Cioffi R, Farina I, Fraternali F, et al. Epoxy/glass fibres composites for civil applications: comparison between thermal and microwave crosslinking routes. Compos Part B 2017;126:100–7.
[3] Feo L, Latour M, Penna R, Rizzano G. Pilot study on the experimental behavior of GFRP-steel slip-critical connections. Compos Part B 2017;115:209–22.
[4] Ascione F, Feo L, Lamberti M, Penna R. Experimental and numerical evaluation of the axial stiffness of the adhesive connections in composite beams. Compos Struct 2017;176:702–14.
[5] Alecci V, Misseri G, Rovero L, Stipo G, De Stefano M, Feo L, et al. Experimental investigation on masonry arches strengthened with PBO-FRCM composite. Compos Part B 2016;100:228–39.
[6] Acciai A, D'Ambrisi A, De Stefano M, Feo L, Focacci F, Nudo R. Experimental response of FRP reinforced members without transverse reinforcement: failure modes and design issues. Compos Part 2016;89:397–407.
[7] Caporale A, Feo L, Luciano R. Eigenstrain and Fourier series for evaluation of elastic local fields and effective properties of periodic composites. Compos Part B 2015;81:251–8.
[8] Barretta R, Feo L, Luciano R, de Sciarra FM. Application of an enhanced version of the Eringen differential model to nanotechnology. Compos Part B 2016;96:274–80.
[9] Barretta R, Feo L, Luciano R, de Sciarra FM, Penna R. Functionally graded Timoshenko nanobeams: a novel nonlocal gradient formulation. Compos Part B 2016;100:208–19.
[10] Madyan OA, Fan M, Feo L, Hui D. Enhancing mechanical properties of clay aerogel composites: an overview. Compos Part B 2016;98:314–29.
[11] Barretta R, Feo L, Luciano R, de Sciarra FM. A gradient Eringen model for functionally graded nanorods. Compos Struct 2015;131:1124–31.
[12] Kim DH, Kim HS. Waterproof characteristics of nanoclay/epoxy nanocomposite in adhesively bonded joints. Compos Part B 2009;55:86–95.
[13] Ascione F, Feo L, Maceri F. An experimental investigation on the bearing failure load of glass fibre/epoxy laminates. Compos Part B 2009;40(3):197–205.
[14] Ascione F, Feo L, Maceri F. On the pin-bearing failure load of GFRP bolted laminates: an experimental analysis on the influence of bolt diameter. Compos Part B 2010;41(6):482–90.
[15] Friedrich SM, Wu AS, Thostenson ET, Chou TW. Damage mode characterization of mechanically fastened composite joints using carbon nanotube networks. Compos Part A 2011;42(12):2003–9.
[16] Tang Y, Zhou Z, Pan S, Xiong J, Guo Y. Mechanical property and failure mechanism of 3D Carbon–Carbon braided composites bolted joints under unidirectional tensile loading. Mater Des 2015;65:243–53.
[17] Li W, Cai H, Li C, Wang K, Fang L. Micro-mechanics of failure for fatigue strength prediction of bolted joint structures of carbon fiber reinforced polymer composite. Compos Struct 2015;124:345–56.
[18] Zhou S, Sun Y, Ge J, Chen X. Multiaxial fatigue life prediction of composite

bolted joint under constant amplitude cycle loading. Compos Part B 2015;74:131–7.
[19] Scarselli G, Castorini E, Panella FW, Nobile R, Maffezzoli A. Structural behaviour modelling of bolted joints in composite laminates subjected to cyclic loading. Aerosp Sci Technol 2015;43:89–95.
[20] Khashaba UA, Aljinaidi AA, Hamed MA. Analysis of adhesively bonded CFRE composite scarf joints modified with MWCNTs. Compos Part A 2015;71:59–71.
[21] Jakubinek MB, Ashrafi B, Zhang Y, Martinez-Rubi Y, Kingston CT, Johnston A, et al. Single-walled carbon nanotube–epoxy composites for structural and conductive aerospace adhesives. Compos Part B 2015;69:87–93.
[22] Srivastava VK. Effect of carbon nanotubes on the strength of adhesive lap joints of C/C and C/C–SiC ceramic fibre composites. Int J Adhes Adhes 2011;31(6):486–9.
[23] Gude MR, Prolongo SG. Gomez-del Rio T, Urena A. Mode-I adhesive fracture energy of carbon fibre composite joints with nanoreinforced epoxy adhesives. Int J Adhes Adhes 2011;31(7):695–703.
[24] Thostenson ET, Chou TW. Carbon nanotube-based health monitoring of mechanically fastened composite joints. Compos Sci Technol 2008;68(12):2557–61.
[25] Ebadi-Dehaghani H, Khonakdar HA, Barikani M, Jafari SH. Experimental and theoretical analyses of mechanical properties of PP/PLA/clay nanocomposites. Compos Part B 2015;69:133–44.
[26] Chan M, Lau K, Wong T, Ho M, Hui D. Mechanism of reinforcement in a nanoclay/polymer composite. Compos Part B 2011;42(6):1708–12.
[27] Subramaniyan AK, Sun CT. Enhancing compressive strength of unidirectional polymeric composites using nanoclay. Compos Part A 2006;67(12):2257–68.
[28] Heydari-Meybodi M, Saber-Samandari S, Sadighi M. A new approach for prediction of elastic modulus of polymer/nanoclay composites by considering interfacial debonding: experimental and numerical investigations. Compos Sci Technol 2015;117:379–85.
[29] Gabr MH, Okumura W, Ueda H, Kuriyama W, Uzawa K, Kimpara I. Mechanical and thermal properties of carbon fiber/polypropylene composite filled with nano-clay. Compos Part B 2015;69:94–100.
[30] Yasmin A, Abot JL, Daniel IM. Processing of clay/epoxy nanocomposites by shear mixing. ScriptaMaterialia 2003;49(1):81–6.
[31] Khan SU, Iqbal K, Munir A, Kim JK. Quasi-static and impact fracture behaviors of CFRPs with nanoclay-filled epoxy matrix. Compos Part A 2011;42(3):253–64.
[32] Khan SU, Munir A, Hussain R, Kim JK. Fatigue damage behaviors of carbon fiber-reinforced epoxy composites containing nanoclay. Compos Sci Technol 2010;70(14):2077–85.
[33] Qi B, Zhang QX, Bannister M, Mai YW. Investigation of the mechanical properties of DGEBA-based epoxy resin with nanoclay additives. Compos Struct 2006;75(1):514–9.
[34] Xu Y, Van Hoa S. Mechanical properties of carbon fiber reinforced epoxy/clay nanocomposites. Compos Sci Technol 2008;68(3):854–61.
[35] Wang L, Wang K, Chen L, Zhang Y, He C. Preparation, morphology and thermal/mechanical properties of epoxy/nanoclay composite. Compos Part A 2006;37(11):1890–6.
[36] Iqbal K, Khan SU, Munir A, Kim JK. Impact damage resistance of CFRP with nanoclay-filled epoxy matrix. Compos Sci Technol 2009;69(11):1949–57.
[37] Borrego LP, Costa JDM, Ferreira JAM, Silva H. Fatigue behaviour of glass fibre reinforced epoxy composites enhanced with nanoparticles. Compos Part B 2014;62:65–72.
[38] Eskizeybek V, Avci A, Gülce A. The Mode I interlaminar fracture toughness of chemically carbon nanotube grafted glass fabric/epoxy multi-scale composite structures. Compos Part A 2014;63:94–102.
[39] Fiedler B, Gojny FH, Wichmann MHG, Nolte MCM, Schulte K. Fundamental aspects of nano-reinforced composites. Compos Sci Technol 2006;66(16):3115–25.
[40] Shekar KC, Prasad BA, Prasad NE. Interlaminar shear strength of multi-walled carbon nanotube and carbon fiber reinforced, epoxy–matrix the hybrid composite. Procedia Mater Sci 2014;6:1336–43.
[41] D5961/D5961M-13 Standard test method for bearing response of polymer matrix composite laminates. Composite Materials. ASTM International. West Conshohocken, PA: 7–10.
[42] Karakuzu R, Demirgoren O, Icten BM, Deniz ME. Failure behavior of quasi-isotropic laminates with three-pin loaded holes. Mater Des 2010;31(6):3029–32.
[43] Ozen M, Sayman O. Failure loads of mechanical fastened pinned and bolted composite joints with two serial holes. Compos Part B 2011;42(2):264–74.
[44] Siddiqui NA, Woo RS, Kim JK, Leung CC, Munir A. Mode I interlaminar fracture behavior and mechanical properties of CFRPs with nanoclay-filled epoxy matrix. Compos Part A 2007;38(2):449–60.
[45] Sene TS, Silva LVD, Amico SC, Becker D, Ramirez AM, Coelho LA. Glass fiber hybrid composites molded by RTM using a dispersion of carbon nanotubes/clay in epoxy. Mater Res 2013;16(5):1128–33.
[46] Salimi MN, Merajin MT, Givi MKB. Enhanced mechanical properties of multifunctional multiscale glass/carbon/epoxy composite reinforced with carbon nanotubes and simultaneous carbon nanotubes/nanoclays. J Compos Mater 2016. 0021998316655201.
[47] Pearson RA, Yee AF. Toughening mechanisms in thermoplastic-modified epoxies: 1. Modification using poly (phenylene oxide). Polym 1993;34(17):3658–70.
[48] Quaresimin M, Schulte K, Zappalorto M, Chandrasekaran S. Toughening mechanisms in polymer nanocomposites: from experiments to modelling. Compos Sci Technol 2016;123:187–204.
[49] Ayatollahi MR, Shokrieh MM, Shadlou S, Kefayati AR, Chitsazzadeh M. Mechanical and electrical properties of epoxy/multi-walled carbon nanotube/nanoclay nanocomposites. Iran Polym J 2011;20(10):835–43.
[50] Callister WD, Rethwisch DG. Materials science and engineering. seventh ed. New York: John Willey and Sons Inc; 2007.
[51] Thoppul SD, Finegan J, Gibson RF. Mechanics of mechanically fastened joints in polymer–matrix composite structures–a review. Compos Sci Technol 2009;69(3):301–29.
[52] Aktaş A. Bearing strength of carbon epoxy laminates under static and dynamic loading. Compos Struct 2005;67(4):485–9.